# ADMX SLIC: Results from a Superconducting *LC* Circuit Investigating Cold Axions

N. Crisosto,[*,†,‡] P. Sikivie,[‡] N. S. Sullivan,[‡] and D. B. Tanner[‡]
*University of Florida, Gainesville, Florida 32611, USA*

J. Yang[‡] and G. Rybka[‡]
*University of Washington, Seattle, Washington 98195, USA*

(Received 26 November 2019; revised manuscript received 20 March 2020; accepted 5 May 2020; published 17 June 2020)

Axions are a promising cold dark matter candidate. Haloscopes, which use the conversion of axions to photons in the presence of a magnetic field to detect axions, are the basis of microwave cavity searches such as the Axion Dark Matter eXperiment (ADMX). To search for lighter, low frequency axions in the sub-$2 \times 10^{-7}$ eV (50 MHz) range, a tunable lumped-element *LC* circuit has been proposed. For the first time, through ADMX SLIC (Superconducting *LC* Circuit Investigating Cold Axions), a resonant *LC* circuit was used to probe this region of axion mass-coupling space. The detector used a superconducting *LC* circuit with piezoelectric driven capacitive tuning. The axion mass and corresponding frequency ranges $1.7498–1.7519 \times 10^{-7}$ eV (42.31–42.36 MHz), $1.7734–1.7738 \times 10^{-7}$ eV (42.88–42.89 MHz), and $1.8007–1.8015 \times 10^{-7}$ eV (43.54–43.56 MHz) were covered at magnetic fields of 4.5 T, 5.0 T, and 7.0 T, respectively. Exclusion results from the search data, for coupling below $10^{-12}$ GeV$^{-1}$, are presented.

DOI: 10.1103/PhysRevLett.124.241101

The constituents of the dark matter of our Universe are yet to be accounted for. Axions are a well-motivated dark matter candidate as they arise independently from the Peccei-Quinn solution to the strong *CP* problem [1–3]. If the axion mass is in the $10^{-6}$ to $10^{-5}$ eV range, therefore very long-lived and very weakly coupled, then the cavity haloscope [4,5] appears currently the best detection method. The scheme is based on the electromagnetic coupling of axions to two photons:

$$\mathcal{L}_{a\gamma\gamma} = -g_{a\gamma\gamma} a(x,t) \vec{E}(x) \cdot \vec{B}(x), \tag{1}$$

where $g_{a\gamma\gamma}$ is a coupling constant, $a$ is the axion field, $\vec{E}$ is the electric field, and $\vec{B}$ is the magnetic field. In the presence of a strong magnetic field, an axion may convert into a real, detectable photon. A tuned resonator can subsequently enhance detection of the axion-sourced photon signal. The axion mass is unknown and the detector must be tuned through a range of possible axion masses. The frequency of the axion sourced photon signal, $\omega$, is set by the condition $\hbar\omega \approx m_a c^2 + \frac{1}{2} m_a v^2$, where $m_a$ is the axion mass and $v$ is the axion velocity. The Kim-Shifman-Vainshtein-Zakharov (KSVZ) [6,7] and Dine-Fischler-Srednicki-Zhitnitski (DFSZ) [8,9] models are typically used to set $g_\gamma$ to $\simeq -0.97$ and $\simeq 0.36$, respectively, where $g_{a\gamma\gamma} = g_\gamma(\alpha/\pi f_a)$, $\alpha$ is the fine structure constant, and $f_a$ is the axion decay constant.

Microwave cavity searches, including RBF [10], UF [11], Axion Dark Matter eXperiment (ADMX) [12–16], and HAYSTAC [17], have already scanned sections of axion parameter space. To complement excluded axion mass parameter space, and probe couplings weaker than past helioscope searches [18], a lumped element *LC* circuit structure can be used instead of a microwave cavity [19–21], and was done in the pilot experiment, ADMX SLIC (Superconducting *LC* Circuit Investigating Cold Axions), presented here. This strategy in resonant structure, essentially a new class of contralto haloscopes, is also being pursued by ABRACADABRA [22], BEAST [23], and the Dark Matter Radio Experiment [24]. An optically pumped magnetometer read-out system has also been proposed [25].

If the axion exists, Maxwell's equations are modified to become

$$\nabla \cdot \vec{E} = g_{a\gamma\gamma} \vec{B} \cdot \nabla a \tag{2}$$

$$\vec{\nabla} \times \vec{B} - \frac{\partial \vec{E}}{\partial t} = g_{a\gamma\gamma} \left( \vec{E} \times \vec{\nabla} a - \vec{B} \frac{\partial a}{\partial t} \right). \tag{3}$$

In the presence of a strong static magnetic field $\vec{B}_0$, there is an axion-sourced current

$$\vec{j}_a = -g_{a\gamma\gamma} \vec{B}_0 \frac{\partial a}{\partial t}. \tag{4}$$

Thus, there is a detectable oscillating magnetic field

$$\vec{\nabla} \times \vec{B}_a = \vec{j}_a \tag{5}$$

 

in the quasistatic limit, when the length scale over which the external field $\vec{B}_0$ extends is much smaller than $c/\omega$.

A loop antenna is used to capture the resulting magnetic flux,

$$\Phi_a = -V_m g_{a\gamma\gamma} \frac{\partial a}{\partial t} B_0, \tag{6}$$

where in the case of ADMX SLIC, with a rectangular loop antenna in a solenoid magnet bore, $V_m = \frac{1}{4} l r^2$ is set by the geometry of the primary loop antenna height $l$ and width $r$. Using the definition of inductance it follows that

$$I_a = -\frac{\Phi_a}{L_1} \tag{7}$$

in the limit of infinite capacitance. Including the resonant enhancement results in

$$I_a = \frac{Q}{L_1} V_m g_{a\gamma\gamma} \frac{\partial a}{\partial t} B_0 \tag{8}$$

where $Q$ is the quality factor of the circuit and the time derivative of the axion field relates to local axion density, $\rho_a$, by $\partial a/\partial t = \sqrt{2\rho_a}\sin(m_a t)$. In the case of the experiment described here, $I_a$ is inductively coupled to the input of a first-stage amplifier by a read-out coupling probe. Flux in the read-out coupling probe from mutual inductance, $M$, is given by

$$\Phi_p = M I_a = \kappa\sqrt{L_1 L_2} I_a \tag{9}$$

where $L_1$ is the total inductance of the primary loop antenna and environment parasitics; $L_2$ is the read-out coupling probe inductance, giving a signal power of

$$P_{\text{input}} = \omega\kappa^2 L_1 I_a^2 \tag{10}$$

where $\kappa$ is a coupling constant between $L_1$ and $L_2$.

The pilot experiment ADMX SLIC probes a lower-frequency, lighter-axion mass parameter space that is difficult to reach with existing microwave-cavity axion haloscope searches. Prototype studies led to a NbTi loop antenna capacitively tuned by a piezoelectric-actuated dielectric as a sufficient resonator design [26].

The primary loop antenna of the $LC$ circuit used in our axion search was a single rectangular loop. A single rectangular loop was chosen in order to have large flux capture while keeping mutual inductance and self inductance low as well as for ease of construction. The dimensions of the primary loop antenna were 7.62 cm × 31.25 cm, with copper-matrix-free 0.25 mm diameter NbTi wire strung around a polytetrafluoroethylene (PTFE) form. A parallel plate capacitor was made with 5.08 cm × 5.72 cm NbTi plates, supported by PTFE blocks, and positioned with a 0.464 cm gap between plates. PTFE screws fastened the form and secured the capacitor plates in place. Angle bracket shapes were used for the vertical runs of the form to reduce weight and increase stability. A groove in the PTFE was used to secure most of the NbTi wire; PTFE tape secured the horizontal runs of the form. The NbTi capacitor plates were spot welded to the ends of the NbTi loop. Tuning was achieved by moving an alumina sheet, 5.08 cm × 11.4 cm and 0.152 cm thick, between the parallel plate capacitor with a rotary piezoelectric motor (ANR240). The calculated capacitance was 7.86 pF and 5.53 pF with and without the alumina fully inserted respectively, corresponding to a $\pi/2$ rotation from the piezoelectric motor. Varactor tuning was previously explored here [26,27], but was rejected due to observed high insertion loss. Based on the loop antenna dimensions, the Terman formula [28] estimates an inductance of 0.968 $\mu$H. Given the measured resonant frequency of 42 MHz with the capacitor tuned to its highest value, an effective total inductance, including environment parasitics, of 1.8 $\mu$H is found. The loop antenna is directly mounted to a $^3$He refrigerator. This placement allows for the option of increased cooling in future runs and gives a representation of the resonator performance *in situ* of progressive cryogenic infrastructure.

The magnet used is a Cryomagnetics superconducting (NbTi) solenoid with a 17.1 cm bore and a length of 40 cm. The central field is rated to 8.6 T at a current of 88 A, providing an average field of 7.5 T in a volume of about 8 L. The magnet is supported from a custom made stainless steel vacuum can. The stainless steel vacuum can is lined with a 0.003 in. $Nb_{45}Ti_{55}$ sheet for shielding of the primary loop antenna, tuning, and signal lines from the read-out coupling probe to the first stage amplifier (Stahl amplifier). In the course of data operations the vacuum can was not completely sealed to allow for cooling through immersion from $^4$He. The entire insert, see Fig. 1, is then housed in a superinsulating cryostat made by Precision Cryogenic System, Inc.

For the read-out, a five turn NbTi, PTFE insulated coil was installed to inductively couple to the primary loop antenna. Leads of this read-out coupling probe were connected to the first stage amplifier input by crimping in the CuNi capillary and soldering with PbSn. The highest $Q$ obtained, $Q > 10\,000$, was in this configuration. Comparison of $Q$ in the above described read-out and $Q$ in an alternate configuration of a direct capacitor tap read-out was used to estimate the first stage amplifier input impedance and coupling factor $\kappa$. Area overlap of $L_1$ and $L_2$ was also used to estimate $\kappa$; between the two methods described it is estimated that $\kappa = 0.08 \pm 20\%$.

A low noise cryogenic GaAs FET amplifier [29] is used as the first-stage amplifier. The output of the first-stage cryogenic amplifier above the vacuum can lid is connected via tinned copper braid PTFE insulated coaxial cable to

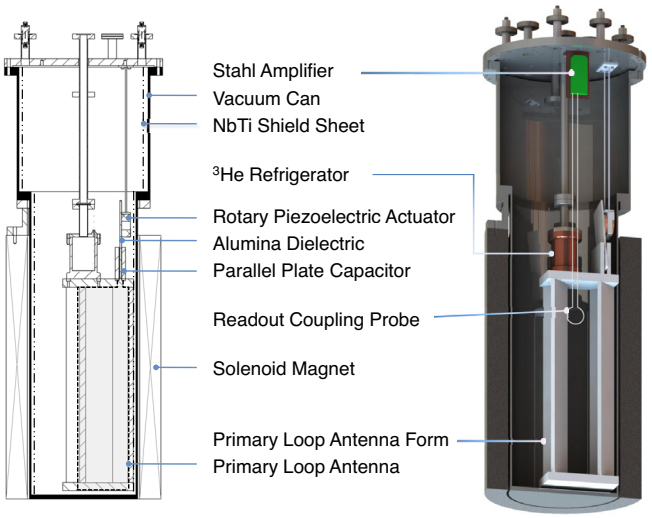


FIG. 1. A sketch of the experiment layout of ADMX SLIC. Two additional weakly coupled probes, for $S_{21}$ measurements and an optional amplifier bypass, are not shown.

room temperature [30]. After postamplification, the signal is fed to a double balanced mixer [31] and heterodyned to 10 kHz. An HP 856A is used as the local oscillator in mixing, controlled by GPIB and LabView drivers. The resulting intermediate frequency (IF) is read by a FFT Spectrum Analyzer (SR760) and written to disk. In between tuning and data taking, a Field Fox Microwave Analyzer N9916A is used to measure $S$ parameters. For $S_{21}$ measurements, white noise power is injected on a weakly coupled stub antenna probe and transmission through the primary loop antenna is measured by the read-out coupling probe. The subsequent transfer function gives $Q$ and resonant frequency. A diagram of the receiver chain is shown in Fig. 2.

From the Friis equation [32], the noise temperature of the experiment is calculated to be 19.7 K [26]. The background spectrum analyzer levels corresponded to Johnson voltage noise fluctuations at 23 K. The greater of the two noise temperature figures is used in the reported analysis.

A reduction of $Q$ and frequency shift was found to track the magnetic field ramp, as shown in Fig. 3. While ramping

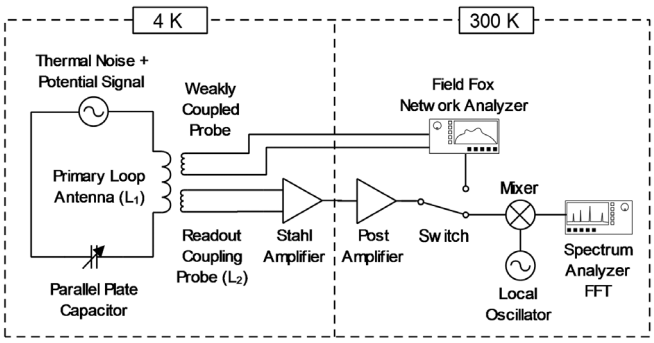


FIG. 2. Receiver chain diagram of ADMX SLIC.

to 4.5 T, the $Q$ was reduced to ~4, 500. At the highest magnetic fields in data operations, $Q$'s were typically 2,200–3,200. Similar in field behavior has been reported in other superconducting resonators and can be attributed to dissipation from the interaction between regions of flux penetration in the superconductor and oscillating currents [33,34].

Data operations consisted of tuning the $LC$ circuit through its full range. At each frequency step, the signal is single heterodyne mixed down to 10 kHz and a FFT spectrum is then taken and digitized with the SR760. An ANR240 rotary piezoelectric motor actuates a mechanical capacitor for the frequency scanning. Between each tuning step, quality factor, resonant frequency, and temperature are measured and recorded.

The FFT spectra were taken with 12.5 kHz spans and 31.25 Hz wide bins. The SR760 used takes 400 points per span and has a real time bandwidth of 100 kHz. Typically, 10 000 averages of 32 ms scans were taken at each frequency and 1 kHz tuning steps were taken between bouts of spectra collection. A tuning range of 42.3–50.0 MHz was expected but in operations was considerably smaller, likely due to the reduction of the piezoelectric effect in low temperature. Intermittently, synthetic signals were injected, on a weakly coupled probe, and observed to verify data taking operations. Run 1 collected data at 4.5 T from 6/16/2018 – 6/19/2018. Run 2 collected data at 5 T and 7 T from 7/19/2018 – 7/27/2018. The signal-to-noise ratio and expected axion sourced power are used to place limits on the coupling of the axion to two photons from the measured power spectra. The signal-to-noise ratio is calculated from the Dicke radiometer equation [35] using power on the input of the first-stage amplifier,

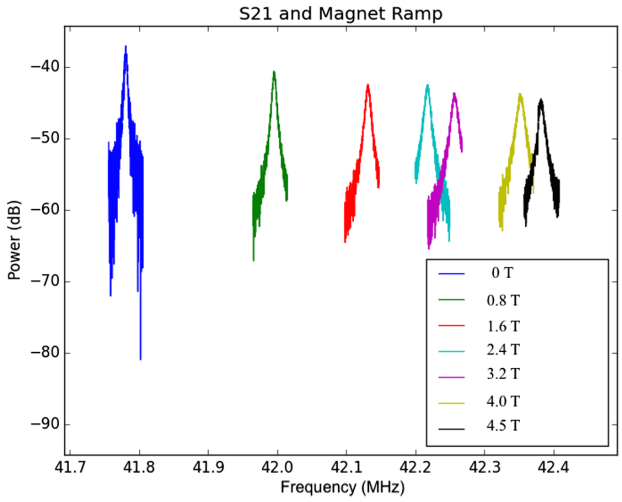


FIG. 3. $S_{21}$ measurements of the loop antenna taken over the course of a magnet ramp. A frequency shift and $Q$ reduction track the increased magnetic field.

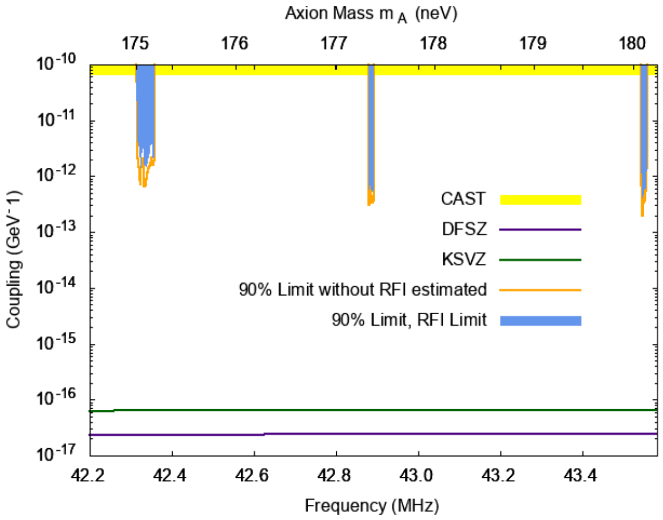


(a) Limit plot from all combined data runs

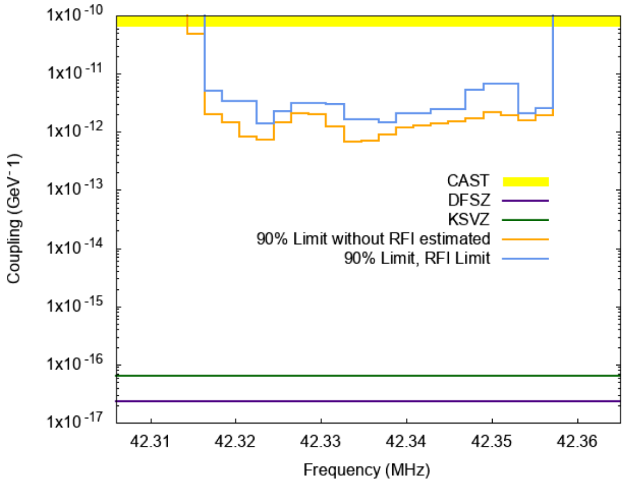


(b) Run 1 with a 4.5 T magnetic field

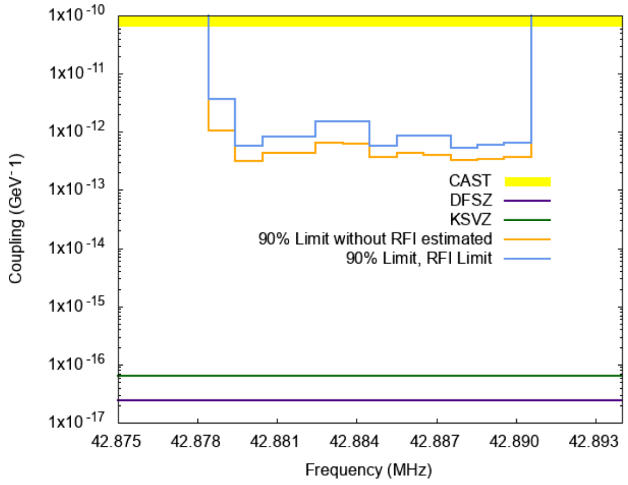


(c) Run 2.a with a 5.0 T magnetic field

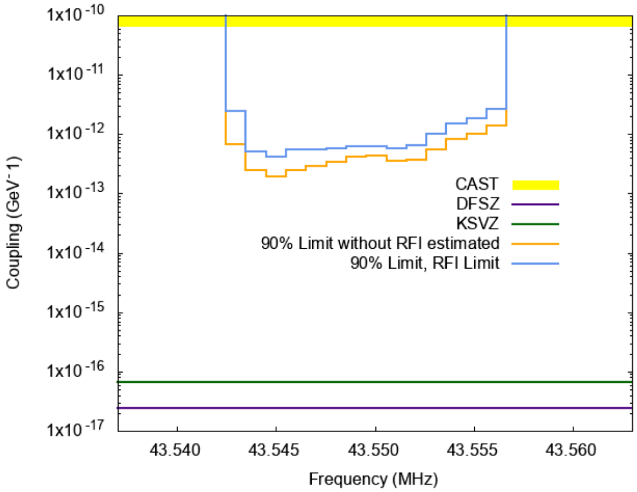


(d) Run 2.b with a 7.0 T magnetic field

FIG. 4. Individual and combined limits collected by ADMX SLIC.

$$\mathrm{SNR} = \frac{P_{\mathrm{input}}}{kT}\sqrt{\frac{\Delta t}{\Delta b}} \tag{11}$$

where $k$ is Boltzman's constant, $T$ is system noise temperature, $\Delta t$ is integration time, and $\Delta b$ is bandwidth. For each raw spectrum 1 kHz was trimmed off the ends before being co-added to form a grand spectrum. Background subtraction was done through a Savitsky-Golay filter. A significant power excess above average noise power could be indicative of an axion conversion signal [11] and a candidate. Numerous peaks of power excess were observed in the raw spectra, which are likely radio frequency interference (RFI) from external sources, but were not rescanned as part of this study. Peaks were observed in the detector output both with the magnetic field off and with the first stage amplifier output disconnected, further supporting that the peaks are RFI. Axion couplings that would produce signals larger than the observed power excesses can be excluded, as shown in the blue lines of Fig. 4. Future large scale experiments will be able to implement more shielding and rescan excesses to distinguish axion signals from RFI; for the purposes of understanding scaling of these experiments, the estimated limits that could have been achieved were RFI candidates eliminated are shown in orange. It is interesting to note that even limited by RFI, unexplored axionlike-particle dark matter parameter space can be excluded. Figure 4 shows the axion-photon coupling exclusions achieved in the experiment, if axions compose all of the dark matter and have a local density of 0.45 $\mathrm{GeV/cm^3}$. Panels 4(b), 4(c), and 4(d) show the individual runs while panel 4(a) shows the regions combined. The previous best limits set by the CERN Axion Solar Telescope (CAST) are also shown. The limits presented rule out axions with couplings greater than the limit line. Systematic uncertainty in these limits are present from the experiment parameters of equation (11), with the largest being the uncertainty of the estimation of $\kappa$, this is however much smaller than the near order of magnitude of uncertainty from the unaccounted RFI.

An $LC$ circuit based axion search presents a promising approach to scan unexplored regions of low-frequency axion parameter space. Extensive prototype testing culminated in a piezoelectric-actuated dielectric-tuned NbTi superconducting $LC$ circuit. The operation of this new form of axion detector tested design considerations for future implementations including the measurements of ac electrical losses in superconducting circuits in a large magnetic field. Our pilot experiment operated in 4.2 K and magnetic fields of 4.5–7 T. The axion mass ranges of $1.7498–1.7519 \times 10^{-7}$ eV (42.31–42.36 MHz), $1.7734–1.7738 \times 10^{-7}$ eV (42.88–42.89 MHz), and $1.8007–1.8015 \times 10^{-7}$ eV (43.54–43.56 MHz) were searched. A large amount of external RF noise was found in the data. Despite an external RFI noise limited analysis, a new section of axion mass and coupling was excluded. Future versions of contralto haloscopes could continue to cover new parameter space; from the execution of the pilot experiment ADMX SLIC, it is evident that particular high return improvements of this type of search include bolstering the tuning mechanism and improving shielding.

Research at the University of Florida has been supported by the US Department of Energy through Grants No. DE-SC0010296 and No. DE-SC0009723TDD. Additional work at the University of Washington is supported by the US Department of Energy through Grant No. DE-SC0011665. The authors gratefully acknowledge useful comments by Gianpaolo Carosi, John Clarke, Joe Gleason, Greg Labbe, Bill Malphurs, and Leslie Rosenberg. The authors also gratefully acknowledge the larger ADMX Collaboration beyond those responsible for this particular work who provided comments on the draft.

*Corresponding author.
nmc25@uw.edu
†Present address: Box 351560, University of Washington Seattle, WA 98195 USA.
‡All of the authors also are members of the ADMX Collaboration and the work reported reflects results obtained by those authors who worked directly on this project related to but distinct from ADMX.

[1] R. D. Peccei and H. R. Quinn, Phys. Rev. Lett. **38**, 1440 (1977).
[2] S. Weinberg, Phys. Rev. Lett. **40**, 223 (1978).
[3] F. Wilczek, Phys. Rev. Lett. **40**, 279 (1978).
[4] P. Sikivie, Phys. Rev. Lett. **51**, 1415 (1983).
[5] P. Sikivie, Phys. Rev. D **32**, 2988 (1985).
[6] J. E. Kim, Phys. Rev. Lett. **43**, 103 (1979).
[7] M. A. Shifman, A. Vainshtein, and V. I. Zakharov, Nucl. Phys. **B166**, 493 (1980).
[8] A. Zhitnitsky, Sov. J. Nucl. Phys. **31**, 260 (1980).
[9] M. Dine and W. Fischler, Phys. Lett. **120B**, 137 (1983).
[10] S. De Panfilis, A. Melissinos, B. Moskowitz, J. Rogers, Y. Semertzidis, W. U. Wuensch, H. J. Halama, A. G. Prodell, W. B. Fowler, and F. A. Nezrick, Phys. Rev. Lett. **59**, 839 (1987).
[11] C. Hagmann, P. Sikivie, N. S. Sullivan, and D. B. Tanner, Phys. Rev. D **42**, 1297 (1990).
[12] S. J. Asztalos, E. Daw, H. Peng, L. J. Rosenberg, D. B. Yu, C. Hagmann, D. Kinion, W. Stoeffl, K. van Bibber, J. LaVeigne, P. Sikivie, N. S. Sullivan, D. B. Tanner, F. Nezrick, and D. M. Moltz, Astrophys. J. Lett. **571**, L27 (2002).
[13] S. J. Asztalos, G. Carosi, C. Hagmann, D. Kinion, K. van Bibber, M. Hotz, L. J. Rosenberg, G. Rybka, J. Hoskins, J. Hwang, P. Sikivie, D. B. Tanner, R. Bradley, and J. Clarke, Phys. Rev. Lett. **104**, 041301 (2010).
[14] J. Sloan *et al.*, Phys. Dark Universe **14**, 95 (2016).
[15] J. Hoskins *et al.*, Phys. Rev. D **94**, 082001 (2016).
[16] N. Du *et al.* (ADMX Collaboration), Phys. Rev. Lett. **120**, 151301 (2018).
[17] L. Zhong *et al.*, Phys. Rev. D **97**, 092001 (2018).
[18] V. Anastassopoulos *et al.* (CAST Collaboration), Nat. Phys. **13**, 584 (2017).

[19] P. Sikivie, N. Sullivan, and D. B. Tanner, Phys. Rev. Lett. **112**, 131301 (2014), see also Ref. [20].
[20] Unpublished work on the LC circuit axion dark matter detector was done in the early 2000s by the authors of Ref. [19] and independently by B. Cabrera and S. Thomas. The work of Cabrera and Thomas was presented in a talk, http://www.physics.rutgers.edu/~scthomas/talks/Axion-LC-Florida.pdf, at the Axions 2010 Conference in Gainesville, Florida, January 15–17.
[21] J. Ouellet and Z. Bogorad, Phys. Rev. D **99**, 055010 (2019).
[22] J. L. Ouellet, C. P. Salemi, J. W. Foster, R. Henning, Z. Bogorad, J. M. Conrad, J. A. Formaggio, Y. Kahn, J. Minervini, A. Radovinsky, N. L. Rodd, B. R. Safdi, J. Thaler, D. Winklehner, and L. Winslow, Phys. Rev. Lett. **122**, 121802 (2019).
[23] B. T. McAllister, M. Goryachev, J. Bourhill, E. N. Ivanov, and M. E. Tobar, arXiv:1803.07755.
[24] M. Silva-Feaver, S. Chaudhuri, H. Cho, C. Dawson, P. Graham, K. Irwin, S. Kuenstner, D. Li, J. Mardon, H. Moseley, R. Mule, A. Phipps, S. Rajendran, Z. Steffen, and B. Young, IEEE Trans. Appl. Supercond. **27**, 1 (2017).
[25] P.-H. Chu, L. D. Duffy, Y. J. Kim, and I. M. Savukov, Phys. Rev. D **97**, 072011 (2018).
[26] N. Crisosto, Searching for low mass axions with an LC circuit, Ph.D. Thesis, University of Florida, 2018.
[27] N. Crisosto, P. Sikivie, N. S. Sullivan, and D. B. Tanner, in *Microwave Cavities and Detectors for Axion Research*, edited by G. Carosi, G. Rybka, and K. van Bibber (Springer International Publishing, Cham, 2018), pp. 127–133.
[28] F. Terman, *Radio Engineers Handbook* (McGraw-Hill, London, 1950).
[29] Stahl HDC-50.
[30] Pasternak PE-SR405FL.
[31] Minicircuits ZX05-1+.
[32] H. Friis, Proc. IRE **32**, 419 (1944).
[33] S. Ulmer, H. Kracke, K. Blaum, S. Kreim, A. Mooser, W. Quint, C. C. Rodegheri, and J. Walz, Rev. Sci. Instrum. **80**, 123302 (2009).
[34] M. S. Ebrahimi, N. Stallkamp, W. Quint, M. Wiesel, M. Vogel, A. Martin, and G. Birkl, Rev. Sci. Instrum. **87**, 075110 (2016).
[35] R. H. Dicke, Rev. Sci. Instrum. **17**, 268 (1946).